

IAA-PDC-23-105

**DIDYMOS AND DIMORPHOS SURFACE AND EJECTA REFLECTANCE
PROPERTIES THROUGH DART AND LICIACube IMAGING**

P. H. Hasselmann⁽¹⁾, E. Dotto⁽¹⁾, J.D.P. Deshapriya⁽¹⁾, G. Poggiali^(2,3), A. Rossi⁽⁴⁾, I. Bertini⁽⁵⁾, G. Zanotti⁽⁶⁾, S. Ieva⁽¹⁾, S. Ivanovski⁽⁷⁾, E. Mazzotta-Epifani⁽¹⁾, V. Della Corte⁽⁸⁾, J. Sunshine⁽⁹⁾, A. Zinzi^(10,11), J-Y. Li⁽¹²⁾, L. Kolokolova⁽¹³⁾, D. Glenar^(14,15,16), R. Lalochi^(14,15,16), M. Amoroso⁽¹¹⁾, O. Barnouin⁽¹⁷⁾, J.R. Brucato⁽²⁾, N. Chabot⁽¹⁷⁾, A. Cheng⁽¹⁷⁾, A. Capannolo⁽¹⁸⁾, S. Caporali⁽¹⁾, M. Ceresoli⁽⁶⁾, B. Cotugno⁽¹⁹⁾, G. Cremonese⁽²⁰⁾, T. R. Daly⁽¹⁶⁾, M. Dall'Ora⁽²¹⁾, V. Di Tana⁽¹⁹⁾, C.M. Ernst⁽¹⁷⁾, T. Farnham⁽⁹⁾, F. Ferrari⁽⁶⁾, I. Gai⁽²²⁾, G. Impresario⁽¹⁰⁾, D. P. Sanchez-Lana⁽²³⁾, M. Lavagna⁽⁶⁾, A. Lucchetti⁽²⁰⁾, F. Miglioretti⁽¹⁹⁾, D. Modenini⁽²²⁾, M. Pajola⁽²⁰⁾, S. Pirrotta⁽¹⁰⁾, P. Palumbo⁽⁵⁾, D. Perna⁽¹⁾, S. Raducan⁽²⁴⁾, A. Rivkin⁽⁹⁾, S.R. Schwartz⁽¹²⁾, S. Simonetti⁽¹⁹⁾, T. J. Stubbs⁽¹⁵⁾, P. Tortora⁽²²⁾, M. Zannoni⁽²²⁾.

Corresponding author: pedro.hasselmann@inaf.it

1-INAf-Osservatorio Astronomico di Roma, Monte Porzio Catone, Roma, Italy; 2-INAf-Osservatorio Astrofisico di Arcetri, Firenze, Italy; 3-LESIA-Observatoire de Paris PSL, Paris, France; 4-IFAC-CNR, Sesto Fiorentino, Firenze, Italy; 5-Università degli Studi di Napoli "Parthenope", Dip. di Scienze & Tecnologie, Centro Direzionale, Napoli, Italy; 6-Politecnico di Milano, Dip. di Scienze e Tecnologie Aerospaziali, Milano, Italy; 7-INAf-Osservatorio Astronomico di Trieste, Trieste, Italy; 8-INAf-Istituto di Astrofisica e Planetologia Spaziali, Roma, Italy; 9-University of Maryland, Department of Astronomy, MD-USA; 10-Agenzia Spaziale Italiana, Roma, Italy; 11-Space Science Data Center – ASI, Roma Italy; 12-Planetary Science Institute, University of Arizona, Tucson, AZ-USA; 13-University of Maryland, College Park, MD-USA, 14-Center for Space Sciences and Technology, University of Maryland, MD-USA; 15-NASA Goddard Space Flight Center, Greenbelt, MD-USA; 16-Center for Research and Exploration in Space Science and Technology, NASA/GSFC, Greenbelt, MD-USA; 17-Johns Hopkins University Applied Physics Laboratory, Laurel, MD-USA; 18-ISAE-SUPAERO, Université de Toulouse, Toulouse, France; 19-Argotec, Torino, Italy; 20-INAf-Osservatorio Astronomico di Padova, Padova, Italy; 21-INAf-Osservatorio Astronomico di Capodimonte, Napoli, Italy; 22-Università di Bologna, Dip. di Ingegneria Industriale, Forlì, Italy; 23-CCAR, The University of Colorado, Boulder, CO-USA; 24-University of Bern, Bern, Switzerland.

Keywords: *DART, LICIAcube, Albedo, Photometry, Imaging*

Introduction: The NASA/DART mission successfully accomplished the first planetary defense test on the 26th September 2022 when it intentionally impacted Dimorphos, the secondary object of the (65803) Didymos binary system. DART demonstrated the capabilities of the kinetic redirection technique. Dimorphos was hit by DART with velocity of 6.1 km/s, which produced a complex ejecta plume composed of filamentary streams extending roughly 10 km from the surface already 45 seconds after impact [1]. Before the impact, the DRACO imager onboard DART provided near-real-time images during the fast approach phase, unveiling the surface of Dimorphos at a very small spatial resolution in a single phase angle of 59°. The first seconds to minutes into the event were witnessed by the LEIA and LUKE instruments of the Italian Space Agency CubeSat LICIAcube [2]. Both cameras captured several hundreds of images during the fly-by maneuver, with the closest approach of about 57 km from Dimorphos and Didymos. The disk-resolved data obtained has the largest phase angle coverage, ranging from 43° to 118°.

Methodology: With this large phase angle coverage and spatial resolution of the target's surface, combined with ancillary data such as trajectories and shape models, it is possible to retrieve the observational geometries necessary for testing photometric reflectance surface models [3,4,5]. The mid-to-high phase angles of these images are suitable for constraining the surface roughness, the asymmetric factor between scattering lobes, and also the single-scattering albedo. We rely on

Variational Bayesian Inference [6] in order to estimate the parameters and their uncertainties.

For the ejecta analysis, we rely on the outputs of dynamical simulations performed using the dynamical integrator LICEI [7] to propagate the ejecta initialized from ejecta scaling laws [8,9] and the optical constants and phase functions from laboratory measurements of analog compositions, in order to understand the grain size distribution, velocity and spatial distribution from the brightness radial distribution derived from LICIAcube observations, as well as the total mass.

To provide support and analyze the broad grain size distribution range expected in the plume, we worked on synthetic images from the combination of two numerical codes covering two different size regimes: (i) The Mishchenko radiative transfer code [10] for Mie-Lorentz scattering distribution (~0.5-80 microns size in visible wavelength range) with Percus-Yevick filling factor correction (called RTT-PM) to model the optically thick portion of the plume; (ii) the Muinonen geometric optics code [11] for diverse particle shapes and sizes higher than 100 microns to a few millimeters. Interactions are only resolved between the optically thick Mie-scattering cloud and the >100 microns particles, without coherence effects.

Results: *Surfaces.* Preliminary tests with the Hapke model [3] on DRACO Dimorphos data reveal a surface with photometric properties similar to other silicate asteroids. We report a preliminary global single-scattering albedo SSA of 0.21±0.03, phase function at

59° of 2.20 ± 0.15 and roughness slope θ of $25 \pm 4^\circ$. Comparison with previous disk-resolved space mission target, indicates that Dimorphos' single-scattering albedo is more akin to Lutetia (M-type, $p_v=0.19$, Vis. SSA = 0.22, $\theta \sim 28^\circ$), and Ida (S-Type, $p_v=0.20$, Vis. SSA=0.22, $\theta \sim 18^\circ$). While Dimorphos comes out more backscatter than both these objects (P(59°)~1.45). Like Ida, the SSA is into the dark-end of S-type asteroids (avg. SSA = $\sim 0.39 \pm 0.05$).

The phase curve of Didymos' was reconstructed using non-saturated filter-calibrated short-exposed LUKE R-plane 34 frames. LUKE and LEIA radiometric calibration are still an on-going process, yet, we paired LUKE reduced magnitude with ground-observations [12,13,14] in order to obtain a wide phase curve over range of 3° to 113° . The phase slope of 0.037 mag/deg and parameters $G1, G2 = \{0.84, 0.05\}$ [15] place Didymos under the average curve for S-type and much closer to the phase curves of C-type asteroids [16]. However, the data spread is still broad enough to prevent drawing final conclusion on which asteroid type the curve points to (Fig. 1).

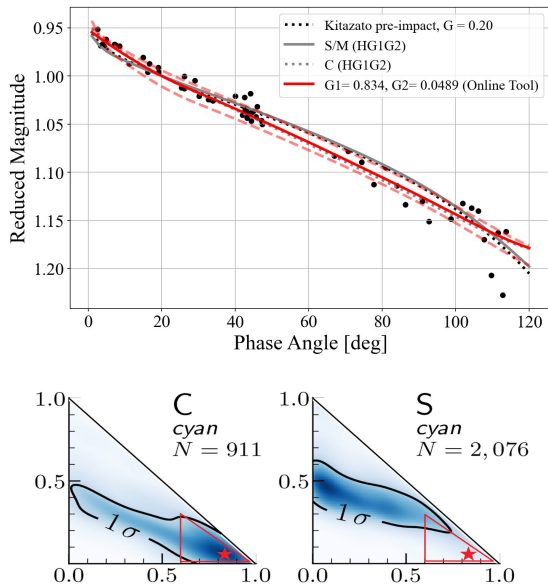


Fig. 1: (top) Didymos phase curve normalized at 20° phase angle. Data under 40° phase angle were collected from literature and are subjected to aspect effects. Red traced lines are the HG1G2 uncertainty envelope (bottom) $G1, G2$ -space with the best solution and uncertainty envelope represented over the PDF for S and C types [17].

Ejecta. Preliminary synthetic images have been produced from LICEI initialized from scaling laws using published parameters [18]. Some morphological features of the ejecta are qualitatively reproduced, such as the elliptical plume shape at T+90s and the apparent filament-like feature at T+180s due to coupling between observation angle and optical depth (Fig. 2). Matching morphological and radial brightness profile can be used as tool to constrain particle density and velocities for the ejecta by permuting initialization conditions.

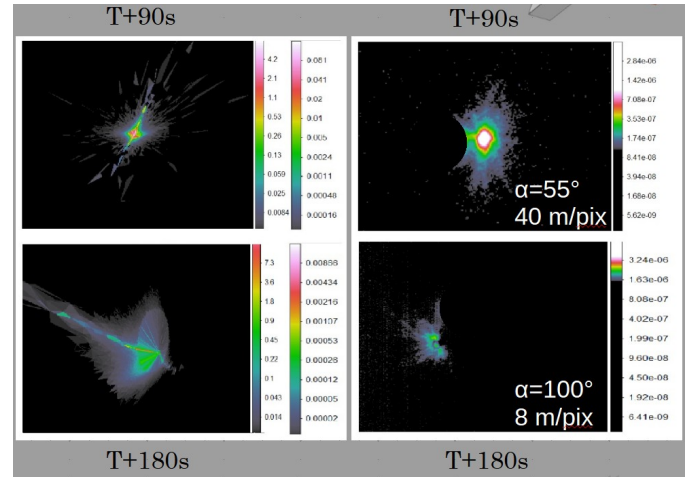


Fig. 2: Examples of synthetic images produced with impact initialization [19] into LICEI [6]. (Left row) the synthetic image color-coded with reflectance and optical depth. (Right row) the filter-calibrated LUKE R-plane image color-coded with uncalibrated signal.

Discussion: Didymos and Dimorphos reflectance properties point to objects with similar composition but situated at the darker-end of the S-type asteroid population. Didymos geometric albedo is ~ 0.15 [19], while S-type generally average in ~ 0.22 . Mix of dark materials and/or shock-darkening can be proposed as albedo suppressors and indicate composition alteration from the LL-Chondrite parent body. Effort is on-going to improve recovering Didymos signal from LUKE and Hapke Modeling Didymos using DRACO images. The ejecta's synthetic imaging remind us of the importance of accounting for geometrical and optical depth effects in producing apparent structures in the plume.

Acknowledgments: This research was supported by the Italian Space Agency (ASI) within the LICIACube project (ASI-INAF agreement AC n. 2019-31-HH.0). This work was supported by the DART mission, NASA Contract No. 80MSFC20D0004.

References: [1] Dotto et al., 2023, Nature, submitted. [2] Dotto et al., 2021, PSS 199. [3] Hapke 2012, 2nd Editon, Cambridge Publisher. [4] Shkuratov et al., 2011, PSS 59. [5] Hasselmann et al., 2016, Icarus 267. [6] Kingma&Welling, 2014, AVBS,1050,1. [7] Rossi et al., 2022, PSJ 3, 118. [8] Zanotti, G., Lavagna, M., (2020), 71st IAC Procc. [9] Housen&Holsapple, 2011, Icar, 211, 856. [10] Mishchenko et al., 2015, JQSRT 156, 97-108. [11] Muinonen et al., 2009, JQSRT 110, 14-16, 1628-1639. [12] Kitazato et al., 2004, LPSC 25, 1623. [13] Pravec et al., 2006, Icarus 181. [14] Pravec et al., 2022, PSJ. [15] Muinonen et al. 2010. [16] Pentilla et al., 2016. [17] Makhler et al., 2021. [18] Fahnstock et al. (2022). [19] Daly et al., 2023, Nature, in press.